frontiers | Frontiers in Materials

TYPE Original Research
PUBLISHED 12 January 2023
DOI 10.3389/fmats.2023.1107133

OPEN ACCESS

EDITED BY
Binbin Mao,
Wuhan University of Technology, China

REVIEWED BY
Bihe Yuan,
Wuhan University of Technology, China
Gang Tang,
Anhui University of Technology, China

*CORRESPONDENCE
Hongming Zhang,
zhanghm@jou.edu.cn

SPECIALTY SECTION
This article was submitted to Energy Materials,
a section of the journal
Frontiers in Materials

RECEIVED 24 November 2022
ACCEPTED 03 January 2023
PUBLISHED 12 January 2023

CITATION
Feng X, Zhang H, Si F, Dou J, Li M, Wu L, Wang S and Zhao L (2023), Suppression characteristics of multi-layer metal wire mesh on premixed methane-air flame propagation.
Front. Mater. 10:1107133.
doi: 10.3389/fmats.2023.1107133

Suppression characteristics of multi-layer metal wire mesh on premixed methane-air flame propagation

Xiangrui Feng[1], Hongming Zhang[1,2]*, Fangyuan Si[1], Jiawei Dou[1], Mingxuan Li[1], Long Wu[1], Shengkang Wang[1] and Lanming Zhao[1]

[1]School of Environmental and Chemical Engineering, Jiangsu Ocean University, Lianyungang, China, [2]Jiangsu Institute of Marine Resources Development, Lianyungang, China

Metal wire mesh is widely used in the energy industry for its excellent protective properties as a fire stopping and explosion isolating material. In this study, the suppression characteristics of different layers of metal mesh on the dynamic behavior of premixed methane-air flame propagation were studied experimentally. A high-speed photographic schlieren system was used to photograph the explosion process to capture the changes in the microstructure of the flame, and high-frequency pressure sensors and micro-thermocouple measurements were used to capture the flame explosion pressure and temperature. The experimental results show that the suppression effectiveness of wire mesh is a reflection of the coupling of explosive flame propagation behavior and combustion state in the pipe. Increasing the number of mesh layers and mesh density can destroy the microstructure of the premixed methane-air flame front and hinder the progress of flame propagation. Increasing the number of wire mesh layers will delay the peak time of premixed flame propagation speed and reduce the peak speed values of flame propagation. Wire mesh has a pronounced attenuation effect on premixed flame temperature and explosion overpressure. The maximum flame temperature attenuation rate is 34.99%–60.95%, and the maximum explosion overpressure attenuation rate is 33.70%–74.02%. And the suppression effect is greatly enhanced as the increase of mesh layers.

KEYWORDS

gas explosion, premixed flame, explosion suppression, metal wire mesh, flame propagation

1 Introduction

As one kind of clean energy fuel, methane has been widely used in industrial production and urban life. Its green, safe and efficient utilization is of great significance to the development of the energy industry. And because of its highly flammable and explosive properties, it is highly susceptible to explosive accidents in mining, storage, use, conversion, etc. This will bring systemic damage to the energy industry and seriously threaten industrial process safety and urban public safety.

To prevent and reduce the occurrence of methane explosions and to attenuate the damage caused by explosive hazards, the exploration and development of related explosion suppression technologies have become a very attractive research area. Much experimental and theoretical work is being carried out (Zheng et al., 2018; Wang et al., 2019; Huang et al., 2021; Dong et al., 2022a; Yuan et al., 2022; Zhao et al., 2022). Cao et al. (2017), Cao et al. (2021) revealed the inhibition mechanism of methane explosion flame propagation by ultrafine water mist through experimental and numerical simulation methods. Yang et al. (2020) and Liu et al. (2020)

compared the suppression effect of adding methane-containing oxidizing bacteria and potassium-containing compounds in ultra-fine water mist on methane explosion. Inert gases such as nitrogen (Luo et al., 2018), carbon dioxide (Chen et al., 2019), and heptafluoropropane (Dong et al., 2022b) also perform well in suppressing methane explosion pressure, flame propagation rate, and chemical reaction processes. In addition, the application of new modified powder inhibitors, such as modified fly ash (Guo et al., 2022), modified montmorillonite (Yu et al., 2020), and new composite inhibitors (Sun et al., 2019; Wang et al., 2020; Tang et al., 2021; Li et al., 2022), has likewise demonstrated their inhibition effect on the dynamic behavior of methane explosion.

However, the use of these methods above is often of a single-use nature, which can effectively avoid and mitigate devastating damage in the event of a process system explosion disaster. Some explosions that occur inside the processing pipeline to prevent and stop flame propagation will lack applicability. At the same time, the above methods will also bring more significant pollution to the equipment and facilities, especially pipelines, vessels, and other process systems, affecting the continuity of the production process. Kundu et al. (2016), Kundu et al. (2017) summarized the premixed methane-air explosion occurrence and flame acceleration. Obstacles and their geometries were found to be potential risk factors for the deflagration-to-detonation transition (DDT) process. And it was proposed that special safety devices should be installed to prevent the transition from methane deflagration to DDT explosion in pipelines. Porous media is often used as a core component of safety devices such as flame arrestors due to its small size, lightweight, good quenching, and other advantages. AL-Zuraiji et al. (2019) found that such online flame arresters have distinct advantages in stopping methane explosion flame propagation and reducing the risk of deflagration to deflagration transition. Nie et al. (2016) analyzed the explosion suppression effect of different foam ceramics. They found that foam ceramics with larger pores have a better impact on the suppression of methane explosion energy. Also, due to its high thermal conductivity, the thickness factor becomes the main influencing factor for suppressing methane explosion. Zhuang et al. (2020) evaluated the sintering resistance of three porous materials, Al_2O_3, SiC, and Fe-Ni alloys, in methane explosion suppression. It was proposed that the sintering resistance, impact resistance, and corrosion resistance of the explosion suppression materials should be considered comprehensively. Wang et al. (2021) and Lu et al. (2021) experimentally investigated and found that metal wire meshes were more effective in suppressing jet fires caused by methane explosions. It was also pointed out that the initial methane concentration, initial pressure, ignition energy, and vent location were essential factors affecting the suppression effect of wire mesh. Cheng et al. (2020), Cheng et al. (2022) analyzed the quenching process of explosion flame through wire mesh by combining large-eddy simulations with experiments. They emphasized that a screen structure in the process piping is effective in preventing the propagation of explosion flame and reducing accidental losses. However, it was also found that there is an increased risk of methane combustion reaction after the flame passes through the screen. In addition, Jin et al. (2020), Jin et al. (2021), Zhang et al. (2016), and Cui et al. (2017) also pointed out that in the explosion-proof design of process piping, the combined effect of the number of mesh layers and mesh numbers should be considered simultaneously to determine the explosion suppression structure.

The above studies show that although wire mesh can be used as a blast suppression material to inhibit the propagation of methane explosions, the safety of its application is constrained by numerous factors and needs to be rigorously demonstrated. In this work, the multi-layer wire meshes are selected as the research object of explosion suppression materials. The microscopic flame structure changes of methane-air explosion flame through different layers of wire mesh, as well as the change rule of the characteristic parameters on explosion dynamics, are comprehensively explored. The process of its suppression effect was analyzed, and its safety protection use in industrial applications was discussed simultaneously.

2 Experimental apparatus and materials

2.1 Experimental apparatus and parameter setting

The methane-air explosion test system is mainly composed of seven parts: explosion pipeline, gas distribution system, high-pressure ignition system, sensing test system, data acquisition system, high-speed schlieren system, and synchronous control system, as shown in Figure 1. The explosive pipe is a stainless steel rectangular tube with explosion-proof structure, and its size is 80 mm × 80 mm × 500 mm. Optical windows are opened at the front and rear sides of the pipe to observe the flow field of explosion flame by installing antiknock quartz glass. The left side of the tube is the air inlet, which is respectively connected to the vacuum pump and the air mixing device, and the right side is the explosion vent. The polypropylene film shall be used for sealing before the test. And then, the configured concentration of premixed methane-air gas is fed to restore the standard air pressure to form an explosive test environment. High-pressure ignition pins, wire mesh, micro-fine thermocouples, and high-frequency pressure sensors (PCB-113B21) are installed in different parts of the pipeline. The detailed parameters of the pipeline are shown in Figure 2. The high-voltage ignition equipment is connected to the ignition pins, and an electric spark is formed at the ignition pins through pulse discharge. The discharge voltage is 14 kV, and the discharge duration is 0.1 s. The high-speed acquisition card in the data acquisition equipment (HOIKI 8861-50) is connected to the thermocouples and pressure sensor, which is responsible for recording the temperature and pressure data of the explosion flame. The data acquisition rate is 20 μ S/s and the recording duration is 1 s. The micro thermocouple used is the R-type thermocouple, which is made of two metal wires welded with a diameter of 25 μm Pt and Pt/Rh13%. The measurement range is from 0°C to 1300°C. The schlieren test system is used in conjunction with a high-speed camera to quickly and accurately capture the changes in the flow field of the explosion flame through the wire mesh structure. The frame rate of the high-speed camera is 20,000 frames/s. A programmable synchronous controller is used to connect high-voltage ignition equipment, high-speed camera, and synchronous data acquisition equipment to achieve trigger and timing control of each device. To ensure the accuracy of the experiments, five parallel experiments are conducted under each experimental condition. If the results obtained for one group of data are significantly different from the other groups and exceed 5%, then it is judged that there is a significant error and this group of data will be excluded. It is necessary to add another group of parallel tests, and the final data results are valid if the error is less than 5%. The

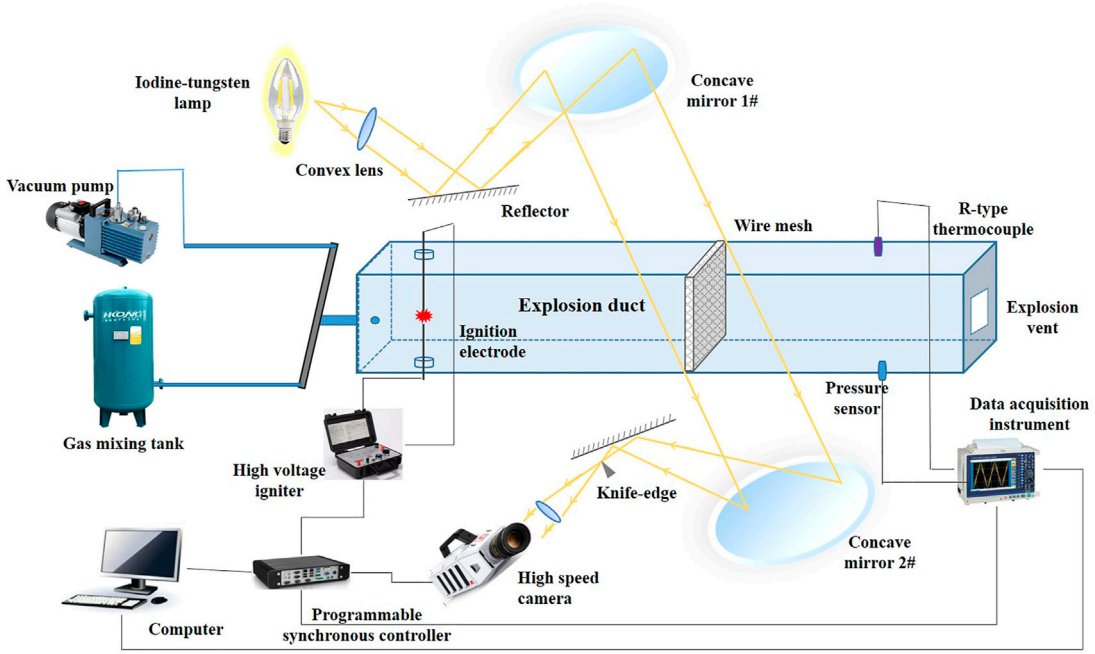

FIGURE 1
Experimental apparatus of gas explosion test system.

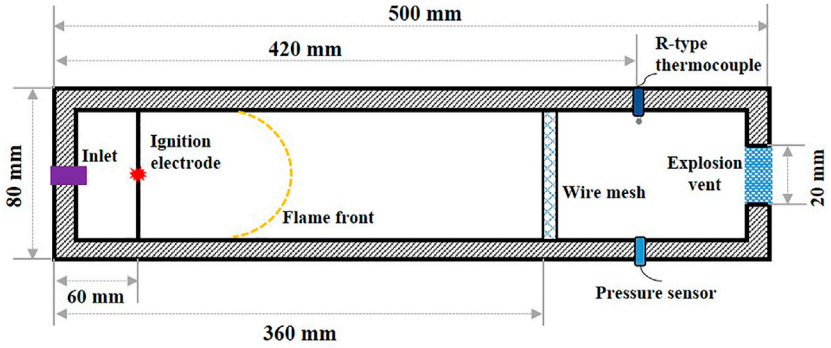

FIGURE 2
Detailed parameter diagram of explosion duct.

final data results provided are those of tests that are closest to the average value of the data in each group.

2.2 Experimental materials

Methane-air premixed gas under a stoichiometric ratio (methane volume fraction is 9.5%) was selected as the explosive gas environment. The initial test pressure is 101.3 kPa, and the initial temperature is 298K. The 40 mesh wire mesh with layers 1, 3, and 5 was selected as the explosion suppression device, which was installed 360 mm away from the starting point of the pipeline. The wire mesh is prepared by multiple metal wires and is made of 304 stainless steel. Before the experiment, the multi-layer wire mesh was fixed together by overlapping the clamping apparatus and then placed in the corresponding position of the pipe. The physical and model diagrams are shown in Figure 3. The relationship between the mesh volume and the layer number, mesh, and wire diameter after the multi-layer mesh setup can be expressed by the following equation (Jin et al., 2021).

$$V_M = \frac{1}{2} N \pi d^2 l \left(\frac{l \cdot M}{25.4} + 1 \right) \quad (1)$$

Where V_M is the volume of the multi-layer wire mesh, mm^3; N is the number of wire mesh layers; d is the wire diameter of the wire, mm; l is the cross-sectional area of the pipe, mm^2; and M is the number of wire mesh. Table 1 shows the parameters of the metal wire mesh used in the experiment.

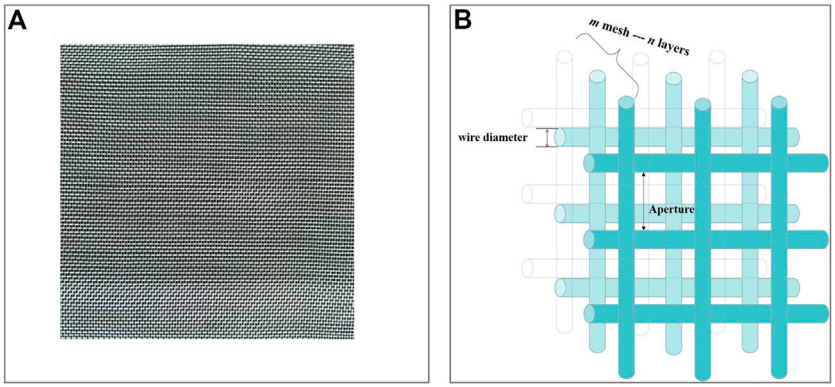

FIGURE 3
Physical and model drawings of wire mesh. **(A)** Physical image, **(B)** Model drawing.

TABLE 1 Parameters of experimental metal wire mesh.

No.	Mesh number	Layer number	Wire diameter (mm)	Mesh volume (mm^3)
1	40	1	0.15	3.184
2	40	3	0.15	9.552
3	40	5	0.15	15.920

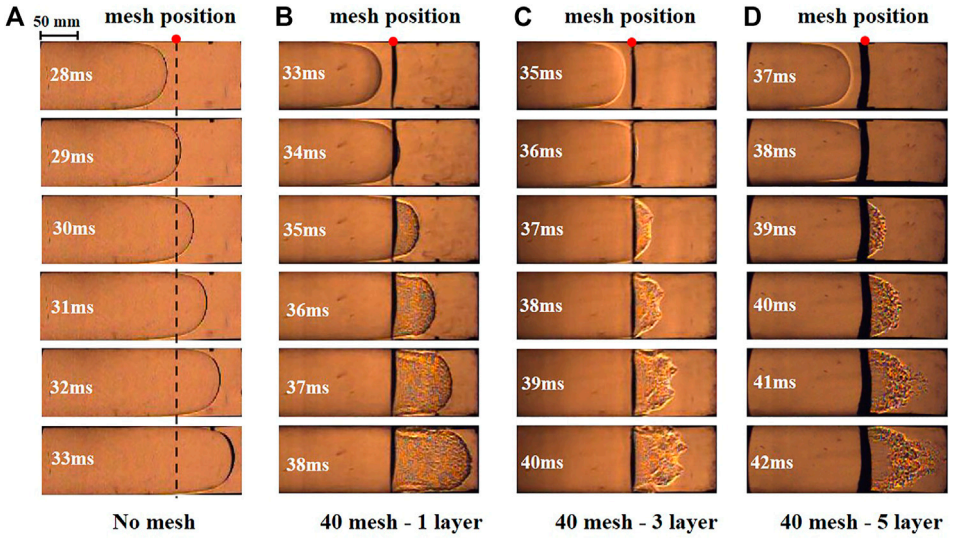

FIGURE 4
Microstructure diagrams of methane-air explosion flame propagation. **(A)** No mesh, **(B)** 1 layer, **(C)** 3 layer, **(D)** 5 layer.

3 Results and discussion

3.1 Effect on flame microstructure

Figure 4 shows the high-speed schlieren dynamic diagrams of premixed methane-air flame without wire mesh and after passing through 40 mesh 1, 3, and 5 layers of metal wire mesh, respectively. The position of the mesh setup is marked in the figure, and at the left end of the position is the evolution of the flame propagating freely in the pipe. At the right end of the position is the microstructural change of the explosion flame after it passes through the metal wire mesh. As shown in Figure 4A, the free propagation of the explosion flame in the semi-closed pipe shows a finger-shaped flame structure. The front end of the flame has a thin, smooth frontal structure, that is, the flame combustion reaction zone, manifested as a laminar combustion process. This follows the typical kinetic stages of premixed flame

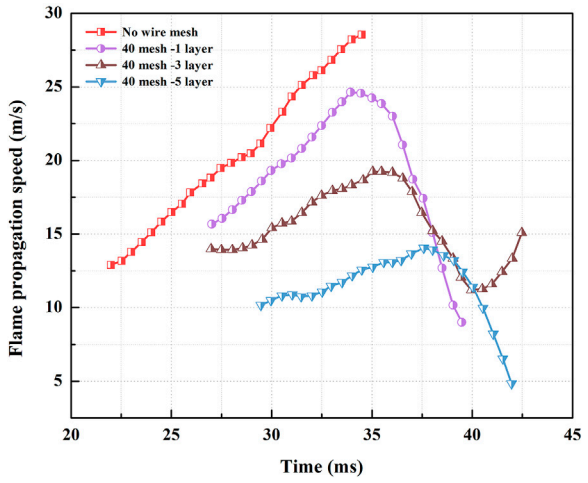

FIGURE 5
Flame front propagation velocity under different wire mesh layers.

propagation proposed by Clanet and Searby (1996). Observing Figures 4B–D, it is found that the flame shows the same finger-shaped flame structure before encountering the wire mesh, which is similar to the case without the wire mesh. However, the curvature of the fronts is reduced by the blockage of the wire mesh, and the blocking effect delays the flame reaching the wire mesh to a certain extent.

When the flame traverses the wire mesh, different layers of wire mesh exhibit different effects on the flame microstructure. As seen in Figure 4B at 35 ms–38 ms, after the flame passes through 1 layer of wire mesh, the flame front is split into several fine strips by the cutting action of the wire mesh. Small folds consistent with the screen structure appear within the flame flow field, but the flame front remains intact and propagates forward in a finger-shaped flame. Observing the variation of 37 ms–40 ms in Figure 4C, when the number of mesh layers is increased to 3, the flame front profile remains intact, but the flame front is seriously distorted. The flame propagation completely loses its finger-shaped propagation structure, and an extensive range of folds appear inside the flame, with turbulent combustion phenomena. At 39 ms–40 ms in Figure 4D, the structure of the 5-layer mesh has wholly shredded the laminar flame front. The flames exhibit a shattered state after passing through the wire mesh, with many fragments in the flame front and destabilization of the flame structure. When propagation reaches 41 ms, the middle part of the flame front suddenly goes out of control laterally, and the flame structure completely breaks up and spreads and propagates until the fragments become smaller and smaller, transforming towards the extinguishing process. It can be seen from the above phenomenon that the single-layer screen only plays a role in separating and cutting the flame, the interference with the overall structure at the flame front is not apprent, and the flame propagation process is unchanged. As the number of mesh layers increases, the interference of the screen to the flame front gradually increases, destroying the original laminar flow flame structure. Turbulent flame structures are evident in localized regions, while more areas are formed with many debris-like flame structures. These fragmented flames propagate by disorderly diffusion within the flow field. Influenced by the surrounding environment, the flame fragments gradually decrease during their propagation and show a gradual extinction.

3.2 Effect on flame propagation velocity

Figure 5 shows the variation of flame front propagation velocity for different layers of the metal wire mesh. For premixed gas explosion flame propagation in the pipeline, the flame front propagation speed is mainly composed of flame combustion speed at the front and unburned gas flow speed at the front (Jin et al., 2020):

$$\boldsymbol{V} = \boldsymbol{V}_c + \boldsymbol{V}_f \tag{2}$$

Where, v is the flame front speed, m/s; v_c is the flame burning speed, m/s; v_f is the unburned gas flow speed, m/s.

As can be seen in Figure 5, in the pipe without the installation of wire mesh, the explosion flame is accelerated propagation state. The flame quickly through the tube, and the speed increases until it drains out of the tube. Once the wire mesh was set up, the flame propagation speed showed a pattern of increasing and then decreasing. The maximum speed of flame propagation also decreases significantly with the increase in the number of mesh layers, indicating that the mesh structure for the propagation speed of the explosion flame does have a specific suppression effect. And the suppression effect is enhanced as the number of mesh layers increases. Observation of the velocity transformation of the 3-layer screen reveals a re-acceleration in the suppression stage of the flame propagation velocity. This indicates that, in this case, a short acceleration process occurs at the back end of the pipe after the flame has passed through the wire mesh, which is consistent with Cheng et al. (2022).

Figure 6 shows the variation of explosion flame propagation acceleration, while Table 2 also gives the relevant characteristic values of flame propagation velocity. Combined with Figure 6 and Table 2, it can be learned that the mesh structure has little effect on flame propagation before it touches the mesh, which propagates to the end of the pipe with a constant acceleration. The flame propagation velocity all show a gradual increase. In the position close to the wire mesh structure, the flame front is blocked by the wire mesh due to the rise of the blockage rate in the pipe, and the acceleration gradually decreases. After passing through the mesh structure, the flame front is cut and heat exchanged by the wire mesh, the flame front is separated and broken, and the thermal response rate is reduced, leading to a further reduction in flame propagation speed. Meanwhile, as the number of mesh layers increases, the time to reach the maximum flame propagation velocity is delayed, and the peak value decreases accordingly. This is because of the mesh multi-layer overlap. The overall mesh hole becomes smaller, the flame flow space in the screen is reduced, and the degree of being cut by the mesh increases. And the flame contact area with the screen increases, and its heat loss increases, resulting in an enhanced extinguishing effect on the flame. In Figures 6A, C short-duration increase in flame acceleration is found at the end of the flame propagation to the pipe. Combined with the microstructure diagram of the flame here, it is found that, there is strong turbulent combustion inside the flame front. This suggests that the splitting effect of the wire mesh caused a re-mixing of the flame front with the unburned gas at the back end, intensifying the combustion near the end of the pipe and causing a temporary flame acceleration. This phenomenon did not occur in the case of 1-layer and 5-layer wire mesh. For the 1-layer wire mesh, as shown in Figure 6B. Because the mesh structure is single and follows a certain weaving order, it makes the premixed explosive flame pass through only to play a role in dividing the flame front, and its structural influence at the flame front does not

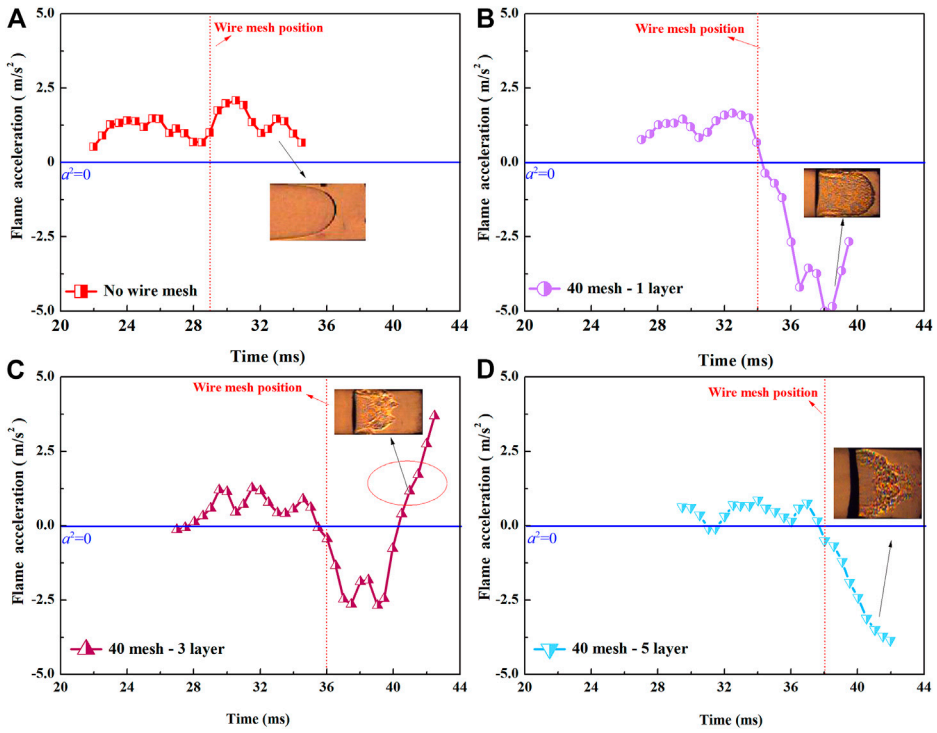

FIGURE 6
Flame acceleration under different wire mesh layers. **(A)** No mesh, **(B)** 1 layer, **(C)** 3 layer, **(D)** 5 layer.

TABLE 2 Characteristic values of flame propagation speed.

Layer number	Acceleration after passing wire mesh (m/s^2)	Maximum flame propagation speed (m/s)	Time of maximum flame propagation speed (ms)
0	0.9937 (>0)	28.56	34.5
1	0.6785 (>0)	24.64	34.0
3	−0.4410 (<0)	19.25	35.5
5	−0.5046 (<0)	14.06	37.5

cause a large turbulent disturbance. Therefore, the flame propagation at this time is only blocked, which weakens the flame propagation speed and has little disturbance to the unburned zone. For the 3-layer wire mesh, the mesh structure not only acts as a barrier to the flame front, but also creates turbulent disturbances in the flame front. It caused the premixed gas in the unburned area to mix fully with the broken flame front and produced a localized acceleration of combustion. The flame propagation rate is influenced by the acceleration of the local combustion reaction and produces an increase in local acceleration. For the 5-layer wire mesh, it is shown in Figure 6D. Due to the stacking and covering of multiple layers of wire mesh, the mesh diameter is too dense. When the flame passes through here, it causes the flame to be split into very small flames after passing through the screen struture, producing a certain degree of quenching. After the unquenched flame passes through the 5-layer mesh, it is also blocked by the cooling effect, and only plays a role in disturbing the flow field of the unburned gas behind the mesh. The combustion reaction at this point is suppressed by the quenching effect, so there is no abnormal feedback of acceleration in this case. This phenomenon does not occur randomly and is related to the mesh structure. It raises a huge warning for our actual process explosion-proof design that the disturbance of the wire mesh to the combustible gases explosive flow field should not be ignored.

3.3 Effect on flame temperature

Figure 7 shows the temperature change of the methane-air explosion flame after passing through different layers of metal wire mesh. The measured temperature data requires data compensation due to thermal inertia at the thermocouple. Assuming that the convective heat transfer process between thermocouple wires is mainly from thermal radiation and heat conduction. The thermocouple temperature correction equation can be expressed as follows (Ballantyne and Moss, 1977).

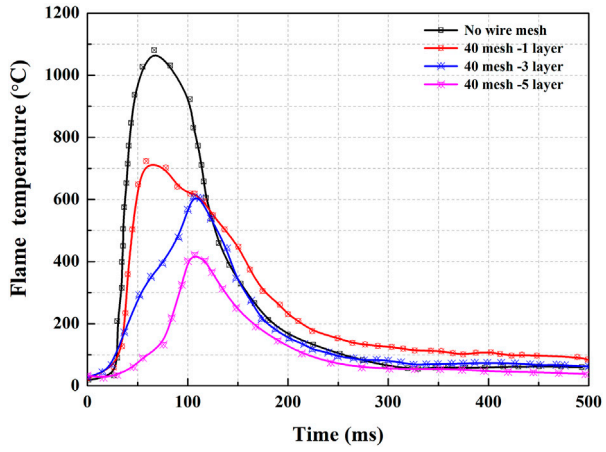

FIGURE 7
Flame front temperature under different wire mesh layers.

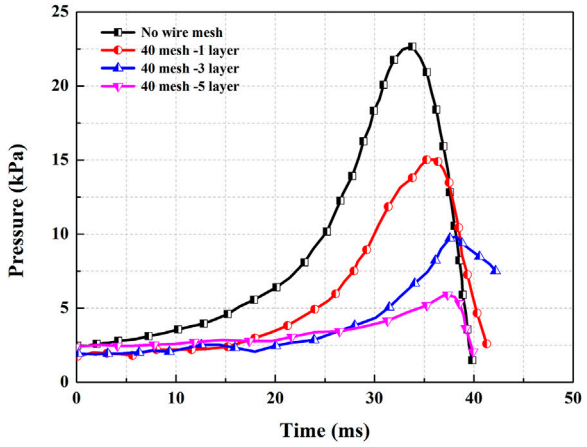

FIGURE 8
Flame explosion pressure under different wire mesh layers.

TABLE 3 Characteristic values of flame temperature.

Layer number	Maximum flame temperature (°C)	Time of maximum temperature (ms)	Maximum temperature decay rate (%)
0	1080.79	66.45	—
1	702.66	78.95	34.99
3	607.41	105.45	43.80
5	422.07	106.95	60.95

$$T = T_m + \tau \frac{dT_m}{dt} \tag{3}$$

Where T_m is the temperature measured by the thermocouple, °C; t is the response time of the thermocouple, ms.

In Figure 7, after the explosion flame passes through the mesh structure, the flame temperature decreases more due to the heat exchange effect. The wire mesh structure has a better attenuation effect on suppressing the flame temperature. Table 3 shows the temperature variation at the monitoring points. According to Figure 7 and Table 3, it can be obtained that the temperature drop of the flame after passing through the wire mesh is noticeable, and its maximum temperature decay rate is improved from 34.99% to 60.95%. As the number of layers increases, the temperature inside the pipe decreases, and the maximum temperature decreases and tends to appear later. It means that the number of mesh layers increases, the flame and metal wire mesh heat transfer are sufficient, and the flame heat loss increases. The better the barrier performance of the flame, the more enhanced the flame temperature attenuation effect.

From the previous section, it can be seen that the wire mesh reduces the speed of the explosion flame front. Thierry and Veynante (2005) pointed out that the laminar burning velocity at the flame front is closely related to the temperature and pressure of the explosion flame propagation process:

$$\frac{S_L}{S_{L_0}} = \left(\frac{T}{T_0}\right)^m + \left(\frac{P}{P_0}\right)^n \tag{4}$$

Where S_L is the flame laminar combustion velocity and S_{L0} is the initial value, m/s; m and n are coefficients of temperature and pressure, respectively (Jin et al., 2017). According to the Arrhenius equation, the effect of temperature on the laminar combustion rate is as follows (Jin et al., 2021):

$$S_L \propto exp\left(-E_a/2RT_f\right) \tag{5}$$

Where E_a is the activation energy, J/mol; R is the ideal gas constant, J/(molK); T_f is the flame temperature, K.

From Eq. 5, the laminar combustion rate of the flame has a high sensitivity to temperature, which means that the chemical reaction rate of the flame is limited by the change in temperature. When the flame contacts the wire mesh, the temperature at the flame front decreases due to the high heat dissipation efficiency of the wire mesh, and the chemical reaction rate of the explosion flame is strongly suppressed. In addition, due to the increase in the number of layers, the rate of heat dissipation increases, which leads to a rise in the rate of temperature decay. For the 3-layer wire mesh structure, the temperature change did not increase due to the re-acceleration of the flame, indicating that this re-acceleration only occurred in a localized area. It did not affect the flame chemical reaction rate change in the entire pipe. Therefore, it can be inferred that the turbulent combustion caused by the flame passing through the wire mesh is small-scale and localized, and the wire mesh has a better effect on the suppression of flame temperature.

TABLE 4 Characteristic values of flame explosion pressure.

Layer number	Maximum explosion pressure (kPa)	Maximum explosion pressure time (ms)	Maximum overpressure decay rate (%)
0	22.67	33.80	—
1	15.03	35.25	33.70
3	9.84	38.23	56.59
5	5.89	37.34	74.02

3.4 Effect on flame explosion overpressure

Figure 8 shows the effect of different layers of wire mesh on the premixed flame explosion overpressure curves. In Figure 8, the maximum explosion overpressure attenuation effect of the 5-layer wire mesh is the strongest in the case of the same number of mesh. The peak value of explosion overpressure is smaller than that of 1-layer and 3-layer wire mesh experiments. Table 4 shows the pressure characteristic values at the monitoring points. For 1-layer wire mesh, the pressure peak can be reached at 33.80 ms, with a maximum pressure peak of 22.67 kPa and a maximum overpressure decay rate of 33.70%. For the 3-layer wire mesh, the peak pressure can be reached at 35.25 ms with a peak pressure of 15.03 kPa and a maximum overpressure decay rate of 56.59%. The pressure depression effect is significantly better than the 1-layer wire mesh case. The increase in the number of wire mesh layers does not delay the time when the explosion pressure reaches its maximum value. It only has the suppressing effect on the maximum pressure value, and the attenuation of pressure by 5 layers is much better than by 1 and 3 layers.

The variation of flame explosion pressure is closely related to the combustion state of the explosion flame in the pipe. And Bychkov and Liberman (2000) gave the relationship between the explosion pressure and the flame flow measurement combustion rate as follows:

$$S_L \propto P^n \tag{6}$$

Where P and n are the pressure and pressure index, respectively. When $n < 0$, the pressure is negatively correlated with the laminar combustion rate; when $n = 0$, the pressure is not associated with the laminar combustion rate; when $n > 0$, the pressure is positively correlated with the laminar combustion rate.

Since the methane concentration in the pipeline is 9.5%, i.e., stoichiometric ratio $\phi = 1$, n > 0 under such conditions (Jin et al., 2020). When the wire mesh is not set, premixed explosion flame pressure and laminar combustion rate promote each other, showing a positive correlation, and the explosion is going to be out of control. When the flame passes through the wire mesh, its flame explosion pressure shows a distinctive decrease, and the laminar combustion velocity decreases with the decay of pressure. The flame behind the wire mesh burns with reduced intensity, leading to further pressure loss. Therefore, the ability of the wire mesh to absorb the explosion pressure wave is the result of the coupled suppression of flame explosion pressure and combustion processes. Due to the combined effect of wire mesh in blocking flame propagation and suppressing gas explosion pressure, it can be used as a enhancement material built into the relevant fire and explosion barrier device at the actual gas explosion site, playing a significant role in the prevention of gas explosion disasters and energy engineering safety protection.

4 Conclusion

In this paper, the microstructural properties and kinetic behaviors of multi-layer wire mesh inside the pipe on the flame propagation of premixed methane-air explosion are experimentally investigated. The wire mesh structures were found to have a splitting and fragmentation effect on the premixed explosive flame. After breaking the flame, its combustion state is changed and gradually changed to the extinguished state by the flow of the flow field. The increase in the number of layers of wire mesh increases the degree of flame fragmentation and dispersion. It is necessary to be alert to the secondary combustion behavior caused by local area turbulence. The wire mesh setting can hinder and slow down the propagation speed of the explosion flame. After flame splitting and crushing by the effect of cooling, there is a marked reduction in flame temperature, and the maximum flame temperature attenuation rate is 34.99%–60.95%. Flame explosion pressure is suppressed by the flame burning rate, with the maximum explosion overpressure attenuation rate of 33.70%–74.02%. In general, the effect of wire mesh on premixed flame overpressure attenuation is better than the attenuation effect on flame temperature, and the more layers of wire mesh on the explosion flame suppression effect is enhanced. Due to the advantages of multi-layer wire mesh in blocking flame propagation and reducing explosion pressure, it has good prospects for application as a gas explosion safety protection material in the energy industry. The results not only reveal the kinetic characteristics of methane-air explosion flame under the action of multi-layer wire mesh but also guide explosion flame suppression in pipelines.

Data availability statement

The original contributions presented in the study are included in the article/Supplementary material, further inquiries can be directed to the corresponding author.

Author contributions

XF, Writing—original draft; HZ, Writing—review and editing; FS, Investigation; JD, Data curation; ML, Formal analysis; LW, Validation; SW, Supervision; LZ, Project administration.

Acknowledgments

The authors gratefully acknowledge the financial supports from the Natural Science Foundation of Jiangsu Province (Grant No.BK20201030), the Natural Science Research Project of Jiangsu Universities (20KJB530013), the Open Research Fund of Jiangsu Institute of Marine Resources Development (Grant No. JSIMR202118), the Jiangsu Province Industry-University-Research Cooperation Project (Grant No. BY2021369) and the Lianyungang Postdoctoral Research Project (LYG2022004).

Conflict of interest

The authors declare that the research was conducted in the absence of any commercial or financial relationships that could be construed as a potential conflict of interest.

Publisher's note

All claims expressed in this article are solely those of the authors and do not necessarily represent those of their affiliated organizations, or those of the publisher, the editors and the reviewers. Any product that may be evaluated in this article, or claim that may be made by its manufacturer, is not guaranteed or endorsed by the publisher.

References

Al-Zuraiji, M. J. A., Zanganeh, J., and Moghtaderi, B. (2019). Application of flame arrester in mitigation of explosion and flame deflagration of ventilation air methane. *Fuel* 257, 115985. doi:10.1016/j.fuel.2019.115985

Ballantyne, A., and Moss, J. B. (1977). Fine wire thermocouple measurements of fluctuating temperature. *Combust. Sci. Technol.* 17 (1/2), 63–72. doi:10.1080/00102209708946813

Bychkov, V. V., and Liberman, M. A. (2000). Dynamics and stability of premixed flames. *Phys. Rep.* 325, 115–237. doi:10.1016/S0370-1573(99)00081-2

Cao, X., Ren, J., Bi, M., Zhou, Y., and Li, Y. (2017). Experimental research on the characteristics of methane/air explosion affected by ultrafine water mist. *J. Hazard. Mater.* 324, 489–497. doi:10.1016/j.jhazmat.2016.11.017

Cao, X., Wang, Z., Lu, Y., and Wang, Y. (2021). Numerical simulation of methane explosion suppression by ultrafine water mist in a confined space. *Tunn. Undergr. Space Technol.* 109, 103777. doi:10.1016/j.tust.2020.103777

Chen, D., Yao, Y., and Deng, Y. (2019). The influence of n2/co2 blends on the explosion characteristics of stoichiometric methane–air mixture. *Process Saf. Prog.* 38, e12015. doi:10.1002/prs.12015

Cheng, F., Chang, Z., Luo, Z., Liu, C., Wang, T., et al. (2020). Large eddy simulation and experimental study of the effect of wire mesh on flame behaviours of methane/air explosions in a semi-confined pipe. *J. Loss Prev. Process Industries* 68, 104258. doi:10.1016/j.jlp.2020.104258

Cheng, F., Lu, J., Li, T., and Luo, Z. (2022). Study on the influence of obstacle on the flame behaviors of methane/air in a semi-confined pipe with wire mesh installed. *J. Loss Prev. Process Industries* 78, 104826. doi:10.1016/j.jlp.2022.104826

Clanet, C., and Searby, G. (1996). On the "tulip flame" phenomenon. *Combust. Flame* 105, 225–238. doi:10.1016/0010-2180(95)00195-6

Cui, Y. Y., Wang, Z. R., Zhou, K. B., Ma, L. S., Liu, M. H., and Jiang, J. (2017). Effect of wire mesh on double-suppression of ch4/air mixture explosions in a spherical vessel connected to pipelines. *J. Loss Prev. Process Industries* 45, 69–77. doi:10.1016/j.jlp.2016.11.017

Dong, Z., Liu, L., Chu, Y., Su, Z., Cai, C., Chen, X., et al. (2022a). Explosion suppression range and the minimum amount for complete suppression on methane-air explosion by heptafluoropropane. *Fuel* 328, 125331. doi:10.1016/j.fuel.2022.125331

Dong, Z., Lv, W., Huang, C., Hao, J., Chen, X., and Liu, L. (2022b). The effects of built-in obstacles on methane-air explosion with concentration gradients: An experimental research. *J. Loss Prev. Process Industries* 78, 104824. doi:10.1016/j.jlp.2022.104824

Guo, C., Jiang, S., Shao, H., Wang, K., and Wu, Z. (2022). Suppression effect and mechanism of fly ash on gas explosions. *J. Loss Prev. Process Industries* 74, 104643. doi:10.1016/j.jlp.2021.104643

Huang, C., Chen, X., Liu, L., Zhang, H., Yuan, B., and Li, Y. (2021). The influence of opening shape of obstacles on explosion characteristics of premixed methane-air with concentration gradients. *Process Saf. Environ. Prot.* 150, 305–313. doi:10.1016/j.psep.2021.04.028

Jin, K., Duan, Q., Liew, K. M., Peng, Z., Gong, L., and Sun, J. (2017). Experimental study on a comparison of typical premixed combustible gas-air flame propagation in a horizontal rectangular closed duct. *J. Hazard. Mater.* 327, 116–126. doi:10.1016/j.jhazmat.2016.12.050

Jin, K., Wang, Q., Duan, Q., Chen, J., and Sun, J. (2021). Effect of metal wire mesh on premixed h2/air flame quenching behaviors in a closed tube. *Process Saf. Environ. Prot.* 146, 770–778. doi:10.1016/j.psep.2020.12.020

Jin, K., Wang, Q., Duan, Q., and Sun, J. (2020). Effect of single-layer wire mesh on premixed methane/air flame dynamics in a closed pipe. *Int. J. Hydrogen Energy* 45, 32664–32675. doi:10.1016/j.ijhydene.2020.08.159

Kundu, S. K., Zanganeh, J., Eschebach, D., Mahinpey, N., and Moghtaderi, B. (2017). Explosion characteristics of methane–air mixtures in a spherical vessel connected with a duct. *Process Saf. Environ. Prot.* 111, 85–93. doi:10.1016/j.psep.2017.06.014

Kundu, S., Zanganeh, J., and Moghtaderi, B. (2016). A review on understanding explosions from methane–air mixture. *J. Loss Prev. Process Industries* 40, 507–523. doi:10.1016/j.jlp.2016.02.004

Li, Y., Chen, X., Yuan, B., Zhao, Q., Huang, C., and Liu, L. (2022). Synthesis of a novel prolonged action inhibitor with lotus leaf-like appearance and its suppression on methane/hydrogen/air explosion. *Fuel* 329, 125401. doi:10.1016/j.fuel.2022.125401

Liu, Z., Zhong, X., Zhang, Q., and Lu, C. (2020). Experimental study on using water mist containing potassium compounds to suppress methane/air explosions. *J. Hazard. Mater.* 394, 122561. doi:10.1016/j.jhazmat.2020.122561

Lu, Y., Wang, Z., Cao, X., Cui, Y., Sun, P., and Qian, C. (2021). Interaction mechanism of wire mesh inhibition and ducted venting on methane explosion. *Fuel* 304, 121343. doi:10.1016/j.fuel.2021.121343

Luo, Z., Su, B., Cheng, F., Wang, T., Shu, C., and Li, Y. (2018). Influences of ethane on the flammable limits and explosive oxygen concentration of methane with nitrogen dilution. *J. Loss Prev. Process Industries* 56, 478–485. doi:10.1016/j.jlp.2018.10.010

Nie, B., Yang, L., and Wang, J. (2016). Experiments and mechanisms of gas explosion suppression with foam ceramics. *Combust. Sci. Technol.* 188, 2117–2127. doi:10.1080/00102202.2016.1218161

Sun, Y., Yuan, B., Chen, X., Li, K., Wang, L., Yun, Y., et al. (2019). Suppression of methane/air explosion by kaolinite-based multi-component inhibitor. *Powder Technol.* 343, 279–286. doi:10.1016/j.powtec.2018.11.026

Tang, G., Liu, M., Deng, D., Zhao, R., Liu, X., Yang, Y., et al. (2021). Phosphorus-containing soybean oil-derived polyols for flame-retardant and smoke-suppressant rigid polyurethane foams. *Polym. Degrad. Stab.* 191, 109701. doi:10.1016/j.polymdegradstab.2021.109701

Thierry, P., and Veynante, D. (2005). *Theoretical and numerical combustion*. Second edition. United States: RT Edwards, Inc.

Wang, L., Liang, Y., Hu, Y., and Hu, W. (2020). Synergistic suppression effects of flame retardant, porous minerals and nitrogen on premixed methane/air explosion. *J. Loss Prev. Process Industries* 67, 104263. doi:10.1016/j.jlp.2020.104263

Wang, T., Luo, Z., Wen, H., Zhang, J., Mao, W., Cheng, F., et al. (2019). Experimental study on the explosion and flame emission behaviors of methane-ethylene-air mixtures. *J. Loss Prev. Process Industries* 60, 183–194. doi:10.1016/j.jlp.2019.04.018

Wang, Z., Lu, Y., Cao, X., Yu, Y., Jiang, J., Jiao, F., et al. (2021). Wire-mesh inhibition of jet fire induced by explosion venting. *J. Loss Prev. Process Industries* 70, 104408. doi:10.1016/j.jlp.2021.104408

Yang, K., Zhang, P., Yue, C., Chen, K., Ji, H., Xing, Z., et al. (2020). Experimental research on methane/air explosion inhibition using ultrafine water mist containing methane oxidizing bacteria. *J. Loss Prev. Process Industries* 67, 104256. doi:10.1016/j.jlp.2020.104256

Yu, M., Wang, X., Zheng, K., Han, S., Chen, C., et al. (2020). Investigation of methane/air explosion suppression by modified montmorillonite inhibitor. *Process Saf. Environ. Prot.* 144, 337–348. doi:10.1016/j.psep.2020.07.050

Yuan, B., He, Y., Chen, X., Ding, Q., Tang, Y., Zhang, Y., et al. (2022). Flame and shock wave evolution characteristics of methane explosion in a closed horizontal pipeline filled with a three-dimensional mesh porous material. *Energy* 260, 125137. doi:10.1016/j.energy.2022.125137

Zhang, S., Wang, Z., Zuo, Q., Jiang, J., and Cheng, C. (2016). Suppression effect of explosion in linked spherical vessels and pipelines impacted by wire-mesh structure. *Process Saf. Prog.* 35, 68–75. doi:10.1002/prs.11728

Zhao, Q., Chen, X., Li, Y., and Dai, H. (2022). Suppression mechanisms of ammonium polyphosphate on methane/coal dust explosion: Based on flame characteristics, thermal pyrolysis and explosion residues. *Fuel* 326, 125014. doi:10.1016/j.fuel.2022.125014

Zheng, L., Li, G., Wang, Y., Zhu, X., Pan, R., et al. (2018). Effect of blockage ratios on the characteristics of methane/air explosion suppressed by bc powder. *J. Hazard. Mater.* 355, 25–33. doi:10.1016/j.jhazmat.2018.04.070

Zhuang, C., Wang, Z., Zhang, K., Lu, Y., Shao, J., and Dou, Z. (2020). Explosion suppression of porous materials in a pipe-connected spherical vessel. *J. Loss Prev. Process Industries* 65, 104106. doi:10.1016/j.jlp.2020.104106